Selective Tight Binding Inhibitors of Trypanosomal Glyceraldehyde-3-phosphate Dehydrogenase via Structure-Based Drug Design

Alex M. Aronov,[†] Christophe L. M. J. Verlinde,[§] Wim G. J. Hol,[§,‡] and Michael H. Gelb*[,†]

Departments of Chemistry, Biochemistry, and Biological Structure, University of Washington, Seattle, Washington 98195, and Howard Hughes Medical Institute, Seattle,Washington 98195

Received April 30, 1998

Glyceraldehyde-3-phosphate dehydrogenase (GAPDH) from the sleeping sickness parasite *Trypanosoma brucei* is a rational target for anti-trypanosomatid drug design because glycolysis provides virtually all of the energy for the bloodstream form of this parasite. Glycolysis is also an important source of energy for other pathogenic parasites including *Trypanosoma cruzi* and *Leishmania mexicana*. The current study is a continuation of our efforts to use the X-ray structures of *T. brucei* and *L. mexicana* GAPDHs containing bound NAD^+ to design adenosine analogues that bind tightly to the enzyme pocket that accommodates the adenosyl moiety of NAD^+. The goal was to improve the affinity, selectivity, and solubility of previously reported 2′-deoxy-2′-(3-methoxybenzamido)adenosine (**1**). It was found that introduction of hydroxyl functions on the benzamido ring increases solubility without significantly affecting enzyme inhibition. Modifications at the previously unexploited N^6-position of the purine not only lead to a substantial increase in inhibitor potency but are also compatible with the 2′-benzamido moiety of the sugar. For N^6-substituted adenosines, two successive rounds of modeling and screening provided a 330-fold gain in affinity versus that of adenosine. The combination of N^6- and 2′-substitutions produced significantly improved inhibitors. N^6-Benzyl (**9a**) and N^6-2-methylbenzyl (**9b**) derivatives of **1** display IC_{50} values against *L. mexicana* GAPDH of 16 and 4 μM, respectively (3100- and 12500-fold more potent than adenosine). The adenosine analogues did not inhibit human GAPDH. These studies underscore the usefulness of structure-based drug design for generating potent and species-selective enzyme inhibitors of medicinal importance starting from a weakly binding lead compound.

Introduction

Sleeping sickness, caused by the protozoon *Trypanosoma brucei*, is considered by the World Health Organization to be one of the main tropical parasitic diseases,[1] in which parasites invade and then freely live in the bloodstream of the mammalian host.[2,3] The disease is fatal if left untreated.[3,4] Existing chemotherapy[3−12] has serious drawbacks, including severe side effects, low efficacy, increasing resistance, and no effect on the most virulent form of sleeping sickness caused by *T. brucei rhodesiense*. Other diseases caused by Trypanosomatidae include leishmaniasis (*Leishmania* genus) and Chagas disease (*Trypanosoma cruzi*).[2,4]

The work presented here focuses on glycolysis in trypanosomes as a target for structure-based drug design. It has been shown that upon going from insect to bloodstream form the parasites become fully dependent on glycolysis for energy production.[2,13,14] Inhibiting glycolysis in parasites would be expected to slow their proliferation, as has been shown by Clarkson and Brohn for the combination of salicylhydroxamic acid and glycerol.[15] Since the kinetic parameters for all of the enzymes in the glycolytic pathway in *T. brucei* are known,[16] it has been possible to simulate parasite glycolytic flux *in computro*.[17,18] Based on the computational result that the presence of a competitive inhibitor of hexokinase at a concentration in the range of $0-K_I$ (K_I is the dissociation equilibrium constant for the E·I complex) has little effect on glycolytic flux, it has been argued that competitive inhibitors of glycolytic enzymes will not be useful for blocking energy production.[18] However, there is no basis for this general statement, as additional simulation studies have shown that glycolytic flux is reduced to 0 in the presence of competitive inhibitors of glyceraldehyde-3-phosphate dehydrogenase (GAPDH) and phosphoglycerate kinase present at $[I]/K_I = 10-100$.[19]

A comparison of the crystal structures of parasite and mammalian glycolytic enzymes forms the basis for rational design of selective inhibitors. Analysis revealed distinct structural differences for GAPDH.[20−23] Glycosomal GAPDH isolated from trypanosomes has been studied previously,[16] and irreversible nonselective inhibitors have been developed.[24]

The adenosyl moiety of NAD^+ does not directly contribute to catalysis and is sufficiently removed from the essential active site cysteine residue, and the amino acid sequence and the position of the protein backbone around it are not completely conserved between human and trypanosomal GAPDH (Figure 1). Significant differences are found next to the conserved *T. brucei* Asp 37 (Asp 34 in human GAPDH) which anchors the adenosine moiety by forming hydrogen bonds to its 2′- and 3′-hydroxyls. In trypanosomal enzymes the backbone is further away from the nucleoside, resulting in

* To whom correspondence should be addressed.
[†] Departments of Chemistry and Biochemistry.
[§] Department of Biological Structure.
[‡] Howard Hughes Medical Institute.

10.1021/jm9802620 CCC: $15.00 © 1998 American Chemical Society
Published on Web 10/31/1998

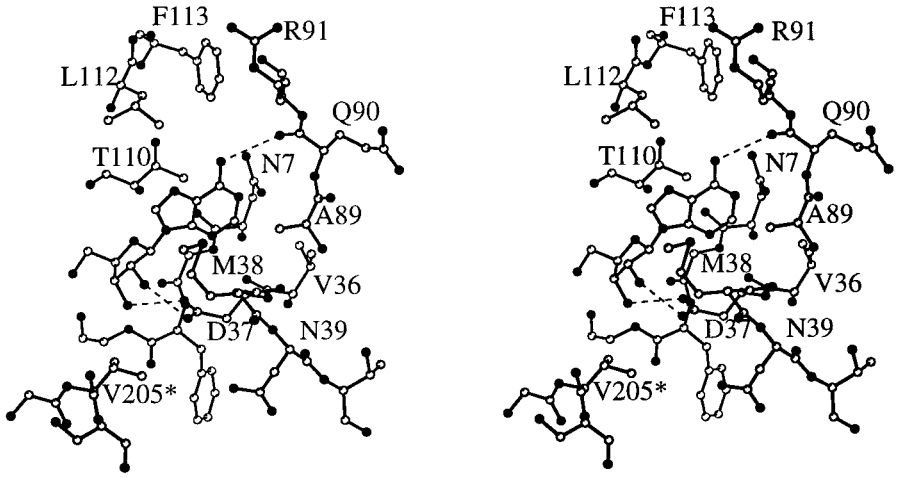

Figure 1. Stereofigure showing the adenosyl moiety of NAD^+ bound to glycosomal *T. brucei* GAPDH. Hydrogen bonds are shown as dashed lines.

Chart 1

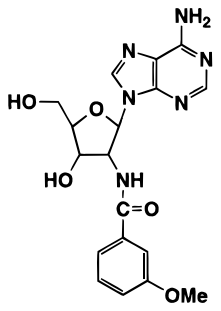

1

a cleft near the 2′-position of the sugar. Flanked by Asn 39 in the *T. brucei* enzyme (Ser 40 in the *L. mexicana* enzyme), this cleft does not exist in the human enzyme because it is essentially filled by Ile 37.[23] This fact was exploited by Verlinde et al.[20,21] who designed, synthesized, and tested a number of 2′-substituted adenosines with adenosine as a lead (IC_{50} value around 50 mM). The best result was achieved with 2′-deoxy-2′-(3-methoxybenzamido)adenosine (**1**) (Chart 1) (IC_{50} values of 0.3 mM for *L. mexicana* GAPDH, 2.2 mM for *T. brucei* GAPDH, and >10 mM for human GAPDH). While using a 2′-amido functional group to preserve the hydrogen bond to the Asp anchor, the design exploited the differences in cleft size and achieved remarkable specificity compared to adenosine, possibly involving a hydrogen bond from the amido function of Asn 39 in *T. brucei* GAPDH to the methoxy oxygen of **1**.

Despite the success in achieving substantial selectivity, the affinity of the best trypanosomal GAPDH inhibitor is still far too low for it to become a valuable drug in treating trypanosomal infections. Attempts to simplify the structure by using cyclopentyl and open-chain adenine derivatives were only marginally successful.[22] The 2′-substituent proved to be incompatible with substituents on the adenine ring such as C^2-methyl[22] or C^8-thienyl,[20] which as monosubstitutions led to a 10- and 180-fold increase in GAPDH affinity, respectively, over adenosine.

In the present study mono- and dimodifications of adenosine have been introduced at positions 2′ and N^6 based on modeling studies. Their effect on GAPDH inhibition has been measured, and optimization was carried out. Inhibitors with significantly higher activity have been obtained. Compatibility of 2′,N^6-disubstitution has been established and should allow for further improvement of the inhibitors currently under study.

Molecular Modeling

Initially, we decided to test the disposition of atoms in the modeled structure of *T. brucei* GAPDH·**1** by adding substituents on the benzamido group at positions that were predicted from the trypanosomal GAPDH X-ray structures not to sterically interfere with binding. Because of the ease of synthesis and possible improvement in solubility, introduction of hydroxyl groups was considered. The proposed binding mode of **1**[20] involves the occupation by a 3-methoxybenzamido group of a mainly hydrophobic and narrow enzyme cleft that starts near the ribosyl 2′-position and widens near Asn 39 (Figure 1). The main recognition features of this substituent are (i) a hydrogen bond between the amide nitrogen and the carboxylate of Asp 37, (ii) sandwiching of the aromatic ring by Met 38 and Val 205* (the latter residue is provided by a neighboring subunit of the GAPDH tetramer), and (iii) a hydrogen bond between the methoxy group and ND2 of Asn 39 (predicted hydrogen bond length 3.3 Å). From inspection of this model it appeared that positions 4 and 5 of the 3-methoxybenzamido were prime candidates for substitution as they were pointing mainly into solvent. Position 2 was also considered, with the possibility of forming an intramolecular hydrogen bond to the 2′-amide nitrogen; such a conformation can be observed in 15 out of 51 2-hydroxybenzamido groups in the Cambridge Crystallographic database with a hydrogen bond length of 2.63 ± 0.04 Å. However, intermolecular contacts did not look favorable since a hydroxyl at position 2 would bump into the OD2 of Asp 37 (predicted distance 2.35 Å). In conclusion, modeling suggested that the introduction of a 4-hydroxyl and a 5-hydroxyl would leave the affinity of **1** unchanged, whereas a 2-hydroxyl would disrupt its binding mode and decrease the GAPDH binding affinity.

The next step was to increase the affinity of our best parasite-selective lead compound **1** by adding substituents to the adenine ring. Because the 8- and 2-substituents discovered during our previous design studies[20] are incompatible with the 2′-(3-methoxybenzamido)

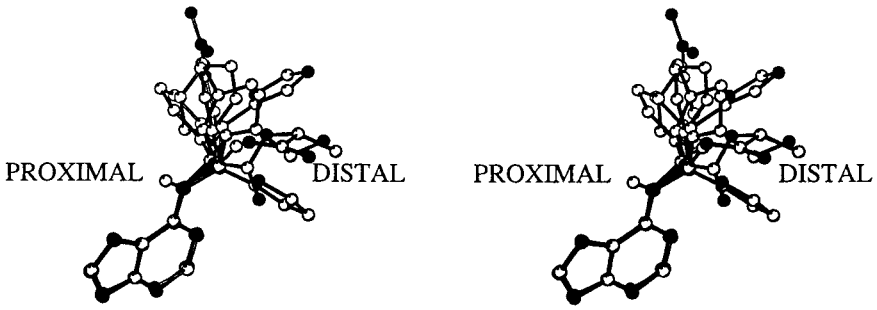

Figure 2. Superposition of the 15 substituted N^6-methyleneadenines present in the Cambridge Crystallographic Database (stereoview). All N^6-substituents are oriented distal with respect to the imidazole of the adenine ring. In contrast, our proposed binding mode in GAPDH has the substituent in the proximal orientation.

moiety due to steric clashes between the introduced substituents,[22] we tried to explore the possibility of introducing substituents at the N^6 position. In proximity to that atom, two hydrophobic clefts exist (Figure 1). One is formed by the side chains of Leu 112 and Phe 113 and the backbone and first two side-chain atoms of Arg 91 (*narrow* cleft). The second site (*wide* cleft) points in the opposite direction and is formed by the side chains of Met 38 and Ala 89 and the backbone of Ala 89. We assayed the *L. mexicana* GAPDH inhibition potency of 11 commercially available N^6-substituted adenosine derivatives that might project a hydrophobic group into the aforementioned clefts. One of the best inhibitors was N^6-benzyladenosine with an affinity for *L. mexicana* GAPDH which was nearly 10-fold higher than that of adenosine. Because a semirandom synthesis of nine more N^6-adenosine derivatives (**7a**−**i**) did not significantly improve on the lead (see Results and Discussion), we decided to pursue derivatization by structure-based inhibitor design methods.

Design was carried out as follows. First, we decided on a synthesis concept of reacting commercially available primary amines with 6-chloropurine riboside. From the Available Chemicals Directory (ACD 95.2), 1124 such compounds were retrieved. After filtering out large compounds (M_r > 250) and compounds with additional reactive functionalities, 88 compounds remained. These were clustered based on their frameworks: 19 mono-, 13 di-, and 3 trisubstituted benzylamines, 22 α-substituted benzylamines, 8 bicyclic compounds, and 23 structures with no apparent similarity to each other. All of the substituents were graphically attached at the N^6-position of the adenosine framework and docked individually into the protein environment. Adenosyl moiety coordinates from X-ray data for NAD^+ were used as a starting point. Each time both the narrow and the wide cleft binding modes were considered for the N^6-substituent. On the basis of steric fit, amount of hydrophobic surface buried, and ease of synthesis, six compounds were selected for synthesis (**7j**−**o**).

It should be noted that in all cases we opted for a C^6−N^6 dihedral angle such that the N^6-substituent was oriented proximal to the imidazole fragment of adenosine in order to avoid severe clashes with the protein backbone of Arg 91. This is in contrast with the distal orientation seen in 15 out of 15 structures in the Cambridge Crystallographic Database, which is usually attributed to avoidance of a steric interference between N^7 of adenosine and the α-methyl(ene) at position N^6 [25] (Figure 2). However, steric interference is not so severe because in none of the doubly N^6-substituted adenosine derivatives in the CSD do the α-methyl(ene) groups at the N^6-position rotate out of the plane of the purine ring. We carried out a semiempirical quantum chemical calculation with the AM1 Hamiltonian on N^6-methyladenine. It indicated that the distal conformation is preferred by only 2 kcal/mol over the proximal one. Hence, we concluded that our proposed binding conformation about C^6−N^6 for the adenosine analogue bound to GAPDH is plausible.

Scheme 1[a]

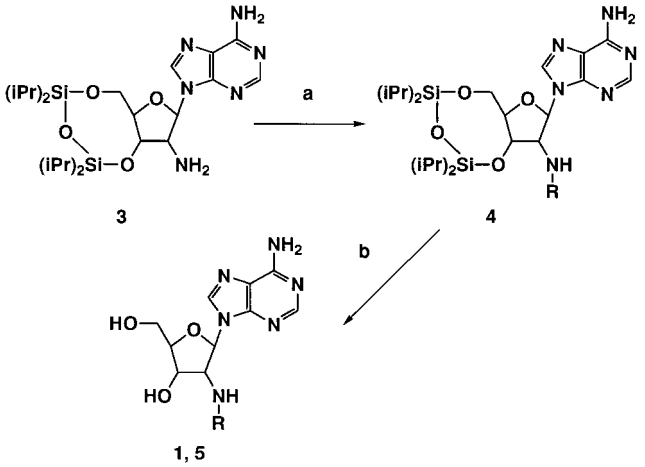

1, 4a: R = 3-methoxybenzoyl
4, 5b: R = 3-methoxy-4-hydroxybenzoyl
4, 5c: R = 2-hydroxy-3-methoxybenzoyl
4, 5d: R = 3-hydroxybenzoyl
4, 5e: R = 3,4,5-trihydroxybenzoyl
4, 5f: R = 3,5-dihydroxybenzoyl

[a] RCOCl, 10:1 CH_2Cl/pyridine; (b) NH_4F, methanol.

Chemistry

Compounds **5b**−**f** were prepared by direct acylation of the Markiewicz-protected 2′-amino nucleoside **3** followed by fluoride-promoted desilylation in MeOH[21] (Scheme 1). Precursor **3** was made from adenine 9-β-D-arabinofuranoside (Ara-A) according to the previously published procedures.[21,26] Hydroxyl functionalities on the benzoyl fragment were protected via $AlCl_3$-catalyzed acetylation[27] prior to activation of the substituted benzoic acids with PCl_5; the acetates were subsequently removed in NH_3/MeOH.

Monosubstituted N^6-alkyladenosines were prepared in a one-step conversion from 6-chloropurine riboside

Scheme 2

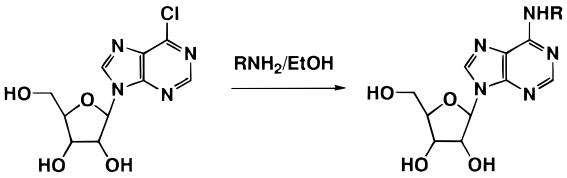

7

7a: R = isopropyl
7b: R = t-butyl
7c: R = n-amyl
7d: R = 2-amyl
7e: R = 2-methylbutyl
7f: R = isoamyl
7g: R = 3-methyl-2-butenyl
7h: R = cyclopentyl
7i: R = cycloheptyl
7j: R = 2-methylbenzyl
7k: R = 3-methylbenzyl
7l: R = 1,2,3,4-tetrahydro-1-naphthyl
7m: R = 1-naphthalenemethyl
7n: R = 2-[2-(hydroxymethyl) phenylthio]-benzyl
7o: R = diphenylmethyl

by nucleophilic substitution with an amine[28,29] (Scheme 2). The only exception was N^6-(3-methyl-2-butenyl)-adenosine. In this case, prenyl bromide was used to alkylate adenosine, and the N^6-alkylated intermediate was rearranged under Dimroth conditions to yield **7g**.[30] To obtain the N^6-isobutyryl derivative **6a**, the protected analogue **4a** was first acylated with isobutyryl chloride and then subjected to NH_4F/MeOH deprotection.

The quickest pathway to 2′,N^6-disubstituted series **9a**−**e** (see Scheme 3) involved subjecting **4a** to alkylation by substituted benzyl bromides with subsequent Dimroth rearrangement, the sequence explored by Robins and co-workers.[30] 2-Methoxy-, 2,5-dimethyl-, and 2,3-dimethylbenzyl bromides were prepared from the corresponding alcohols using PBr_3;[31] 2,3-dimethylbenzyl alcohol was made via $LiAlH_4$ reduction of the respective benzoic acid.[32]

Results and Discussion

Parasite GAPDH and Drug Design. Despite the fact that modeling studies were carried out on GAPDH from *T. brucei*, most of the structure−activity relationship (SAR) work was done with the *L. mexicana* GAPDH, which overexpresses in *Escherichia coli* significantly better than the *T. brucei* enzyme. The amino acid sequences of the two parasite GAPDHs are 81% identical, and the structures of the binding pockets for the adenosyl moiety of NAD^+ are virtually identical except at one position (Asn 39 for *T. brucei* GAPDH and Ser 40 for *L. mexicana* GAPDH). The rms deviation in backbone atoms for the residues in this pocket is 0.2 Å; the rms deviation for the side-chain atoms is 0.5 Å.[33] The conformations of NAD^+ in the two enzymes are also essentially superimposable. In previous studies, it was found that 2′-(3-methoxybenzamido)adenosine analogues typically bind ∼8-fold tighter to *L. mexicana* GAPDH versus *T. brucei* GAPDH.[20] This may be due in part to the Asn 39/Ser 40 difference. In the present study, our better inhibitors of *L. mexicana* GAPDH were also tested on *T. brucei* and *T. cruzi* GAPDHs. The residues comprising the adenosyl binding pockets of the latter two enzymes are identical.

Structure−Activity Relationships. Introduction of hydroxyl groups on the benzamide ring of **1** moderated affinity of the inhibitors for *L. mexicana* GAPDH by less than 4-fold (Table 1). Hydroxyls were tolerated at positions 2−5. The addition of the 2- and 4-hydroxyls led to a minimal improvement in binding: 1.3- and 1.6-fold, respectively. Identical potency of compounds **1** and **5d**, with a 3-OMe and a 3-OH substitution, respectively, most likely argues against the earlier suggestion that **1** benefits from the interaction of its methoxy substituent with Val 207* of the neighboring subunit.[22] However, both groups could possibly form a hydrogen bond to Asn 39 of *T. brucei* GAPDH. The most soluble compound of the series, **5e**, with three hydroxyls on the benzamide, is 3-fold more potent than **1**. Unfortunately, ortho-oxidation is common for gallic acid derivatives,[34] and the resulting *o*-quinone metabolites are highly reactive toward nucleophiles present in the cell.[34,35] To take advantage of both affinity and solubility of **5e**, compound **5f** was synthesized. Its affinity was lower, but the stability was improved. In summary, the effect that different modifications at position 2′ had on inhibitor potency is consistent with our model of the 2′-benzamido moiety occupying the hydrophobic cleft in trypanosomal GAPDHs.

The N^6-position was initially investigated via the testing of commercially available monosubstituted nucleosides. GAPDH binding was selective for secondary amines over amides (Table 2). Compound **6a**, incorporating the isobutyryl moiety, exhibited both decreased affinity and drastically lower solubility as compared to **1**. The screening afforded hits **6b**−**d**, which showed 12−16-fold improvement in binding compared to adenosine (Table 2). They all shared a secondary amine substitution at the N^6-position.

Subsequently we synthesized a series of N^6-substituted adenosine derivatives to explore the use of small aliphatic chains in a semirandom manner. This revealed a clear trend that substituents with more hydrophobic bulk increased binding to GAPDH (see Table 3). Isopropyl (**7a**) and *tert*-butyl (**7b**) chains were too short and thus unable to reach either of the two hydrophobic clefts. Longer chains, both straight and branched close to the nitrogen, had no effect on affinity. As branching moved further away along the chain, binding improved, and the N^6-isoamyl derivative **7f** was the most active noncyclic amine adduct in the series with an IC_{50} of 3.7 mM (10-fold improvement over adenosine). This correlates with the activity of dihydrozeatin riboside (**6d**), as the structures for these two compounds are identical except for the terminal δ-alcohol present in **6d**. Straightening the isoamyl chain by introducing a double bond (**7g**) abbrogated nearly half of the N^6-isoamyl binding contribution. The relative success of adenosines containing N^6-cyclic amines (**7h**,**i**) indicates that flexible cyclic substituents with considerable hydrophobic surface complement the enzyme surface as well as flat aromatic systems.

At this point the N^6-substituent was optimized by using a benzyl substituent as the basis for the second round of drug design. The benzyl moiety provided both the rigid framework and the wealth of structural analogues for further optimization of the N^6-substituent. In an effort to better fill the hydrophobic clefts, compounds **7j**−**o** were synthesized from the amines chosen from the Available Chemicals Directory (see Molecular Modeling) and tested against *L. mexicana* GAPDH. The results are summarized in Table 3. As predicted from modeling, a methyl group introduced at either the ortho- or meta-position on the benzyl ring (**7j**,**k**) improved

Scheme 3[a]

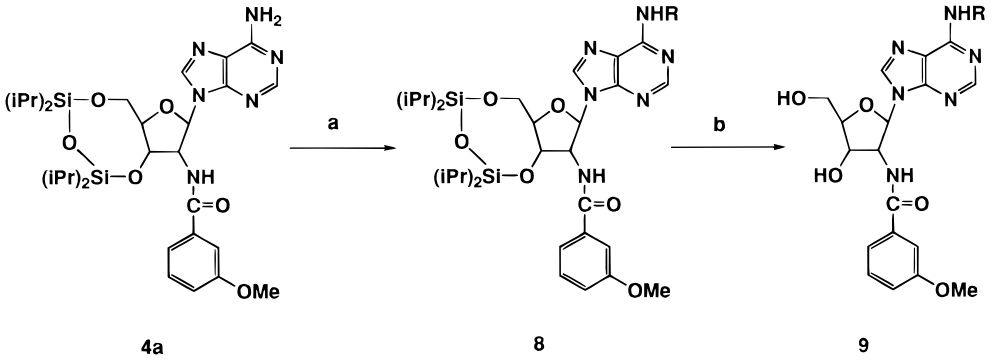

9a: R = benzyl
9b: R = 2-methylbenzyl
9c: R = 2-methoxybenzyl
9d: R = 2,5-dimethylbenzyl
9f: R = 2,3-dimethylbenzyl

[a] (a) RBr, DMF, 45 °C, then *i*Pr-NH_2/methanol (1:3), reflux; (b) NH_4F, methanol.

Table 1. Inhibition of *L. mexicana* GAPDH by 2′-Deoxy-2′-benzamidoadenosine Analogues

	2′-benzamido substituent				
compd	R_2	R_3	R_4	R_5	IC_{50} (μM)
1	H	OMe	H	H	800
5b	H	OMe	OH	H	500
5c	OH	OMe	H	H	600
5d	H	OH	H	H	850
5e	H	OH	OH	OH	250
5f	H	OH	H	OH	650

Table 2. Initial Screening of N^6-Substituted Adenosine Analogues as Inhibitors of *L. mexicana* GAPDH[a]

compd	IC_{50} (μM)
adenosine	50,000[22]
N^6-isobutyryl-2′-deoxy-2′-(3-methoxybenzamido)-adenosine (**6a**)	1,200
N^6-benzyladenosine (**6b**)	4,200
N^6-(4-aminobenzyl)adenosine (**6c**)	3,100
N^6-(4-hydroxy-3-methylbutyl)adenosine (dihydrozeatin riboside) (**6d**)	3,400

[a] K_I values can be calculated from IC_{50} values using the standard formula for competitive inhibition, [NAD^+] = 0.19 mM, and $K_M(NAD^+)$ = 0.4 mM for *L. mexicana* GAPDH, 0.47 for *T. cruzi* GAPDH, and 0.54 for *T. brucei* GAPDH.[36]

inhibition. This can be explained by a further insertion of the substituent into the narrow cleft; molecular mechanics analysis suggests a slight rotation of the side chain of Leu 112 away from Phe 113 as a way to widen the narrow cleft and make favorable interactions possible. Alternatively, partial interaction of benzyl with the narrow cleft and of the methyl with the wide cleft is also possible. Tetraline derivative **7l**, modeled as either *S* or *R* at the new asymmetric center, seemed to cap the narrow hydrophobic cleft rather than enter it. Compound **7m** was the most potent inhibitor in the series (330-fold better than adenosine), most likely by making good van der Waals contacts with the narrow or the wide cleft, but the presence of the naphthalene moiety severely compromised its solubility, which is only 10% higher than its IC_{50} in 5% DMSO/buffer. The aromatic thioether substituent in **7n** seemed, according to our model, to partially expose the second benzene ring to solvent, while **7o** with a diphenylmethyl substituent may take advantage of both hydrophobic clefts.

The combination of N^6-benzyl and 2′-(3-methoxybenzamide) groups on the adenosine scaffold (**9a**) led to a significant improvement in affinity for GAPDH. The IC_{50} of 16 μM is 50-fold lower than that of **1** and 3100-fold lower than that of adenosine, the original lead compound. The modeled binding modes for **9a** are shown in Figure 3. The 2′-substituent fills the selectivity cleft, while the benzyl moiety can occupy either of the two hydrophobic clefts proximal to N^6 of adenosine. There is a synergistic effect with respect to the individual contributions of the substituents (Table 4). Compound **9a** did not detectably inhibit human GAPDH when tested up to its solubility limit of ~0.5 mM. It was shown to be a competitive inhibitor of trypanosomal GAPDH with respect to NAD^+ (Figure 4). Based on the results with **7j**, a 2-methyl group was introduced onto **9a** to give **9b**. This compound is 4-fold more active than **9a**, while retaining its high selectivity for the parasite enzyme; compound **9b** did not inhibit human GAPDH up to 0.27 mM. Despite the fact that human GAPDH also possesses the N^6 pocket, the selectivity for **9a**,**b** is maintained. This selectivity is due to clash of the 2′-benzamido substituent with Ile 37 in the human enzyme, and this will occur when the disubstituted adenosyl moiety sits in the active site of human GAPDH. Other analogues did not show improved potency compared to **9b**. The 2-methoxybenzyl derivative **9c** likely suffered from the putative desolvation of the oxygen upon binding into either of the hydrophobic enzyme clefts. Only an orientation into the narrow cleft appeared possible for **9d**; in the alternative orientation, the methyl in position 5 appeared to bump into the protein backbone of Gln 90. Addition of the 2,3-dimethylbenzyl substitution (**9e**) did not improve binding compared to **9b**, despite the fact that the methyls increase the lipophilicity of the N^6-substituent.

Conclusions

The X-ray structures of *L. mexicana*, *T. brucei*, and human GAPDH·NAD^+ complexes have been used to identify clefts near the adenosyl moiety of NAD^+ that provide opportunity for structure-based inhibitor design. The most potent compound **9b** represents for *L. mexicana* GAPDH a 200-fold improvement over **1** and an

Table 3. Inhibition of *L. mexicana* GAPDH by N^6-Substituted Adenosine Analogues

compd	N^6-R	IC_{50} (μM)
7a		n[a]
7b		n
7c	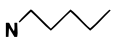	n
7d		n
7e		>5,400 (74%)[b]
7f	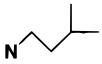	3,700
7g	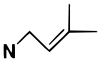	>5,000 (84%)
7h		>5,000 (62%)
7i	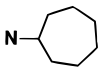	1,800
7j	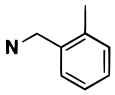	700
7k	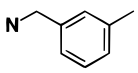	700
7l	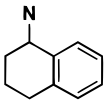	360
7m	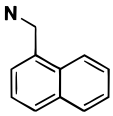	150
7n	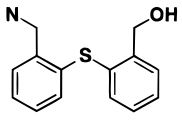	340
7o	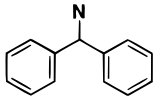	240

[a] Inactive up to 10 mM. [b] Remaining enzyme activity at stated inhibitor concentration.

overall greater than 10^4-fold affinity increase over adenosine. Even though a large number of enzymes use adenosine analogues as cofactors, one could anticipate that highly substituted analogues **9a**−**e** would be rather selective for GAPDH. Compounds such as **9b** are promising antiparasite drug candidates since they may be sufficiently lipophilic to cross parasite membranes in a transporter-independent fashion.

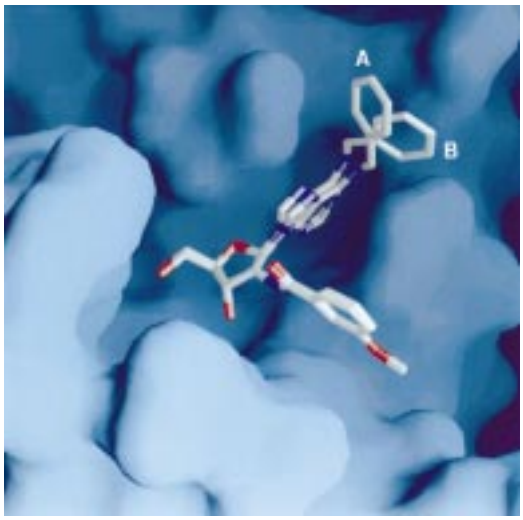

Figure 3. Two possible orientations of the N^6-benzyl substituent of **9a** obtained by molecular modeling. Orientation A fits in the narrow cleft, while B sits in the wide cleft.

Experimental Section

General. Anhydrous solvents were obtained as follows: pyridine was distilled after refluxing overnight with CaH_2 with a $CaSO_4$ dry tube; CH_2Cl_2 was refluxed overnight with P_2O_5 and distilled under Ar; DMF was dried by storing over 4-Å molecular sieves, followed by distillation under reduced pressure. TLC was carried out with precoated silica gel F_{254} plates (EM Science), and spots were detected with UV light (254 nm). Ninhydrin spray was used for detection of amines. Flash chromatography was carried out with silica gel (0.040−0.063 mm; EM Science). NMR spectra were taken on Bruker AF-300 and Bruker WM-500 spectrometers of solutions of ∼2−5 mg of compound in 0.4 mL of $CDCl_3$ unless otherwise mentioned. Electrospray ionization (ESI) mass spectra were obtained on a Kratos Profile HV4 mass spectrometer. All target compounds were shown to be pure by reverse-phase HPLC on C_4 and C_{18} Vydac columns with MeOH/H_2O elution gradient.

Inhibition Studies. (1) Enzymes, Substrates, Cofactors. Recombinant *L. mexicana*, *T. cruzi*, and *T. brucei* glycosomal GAPDHs were obtained as a gift from Drs. H. Kim and P. A. M. Michels.[33,36] NAD^+ and glyceraldehyde-3-phosphate diethyl acetal were purchased from Sigma. Fresh glyceraldehyde-3-phosphate was prepared from its diethyl acetal according to the instructions provided by the manufacturer.

(2) GAPDH Inhibition Assays. The compounds tested were dissolved in DMSO-d_6, and concentrations were determined by integration of NMR peaks with methylene chloride and/or chloroform as internal standards. NMR spectra were collected with a pulse recycle delay of 8 s. The activity of GAPDH was measured in the direction of NADH formation by monitoring absorption at 340 nm at 21 °C. The 0.5-mL reaction mixture contained 0.1 M triethanolamine-HCl buffer, pH 7.6, 1 mM dithiothreitol, 1 mM NaN_3, 5 mM $MgSO_4$, 1 mM EDTA, 10 mM K_2HPO_4, 0.8 mM glyceraldehyde-3-phosphate, and 0.19 mM NAD^+. The concentration of DMSO in the reaction cuvette was kept at 5%. The reaction was started by addition of enzyme. Control reactions were run in the absence of inhibitors but with 5% DMSO. Remaining activity was calculated as percent of control using the initial velocities measured from 0 to 1 min. Inhibitor concentration in the reaction cuvette was varied, with at least five different

Table 4. Selective Parasite GAPDH Inhibition by 2′,N^6-Disubstituted Adenosine Analogues (IC_{50}, μM)

compd	N^6-R	*L. mexicana*	*T. cruzi*	*T. brucei*	human
9a	benzyl	16	159	220	>530 (100%)[b]
9b	2-Me-benzyl	4	30	30	>270 (100%)[b]
9c	2-MeO-benzyl	25	ND[c]	ND	ND
9d	2,5-diMe-benzyl	25	ND	ND	ND
9e	2,3-diMe-benzyl	5.5	ND	ND	ND

[a] All parasite GAPDHs are the glycosomal isoform, and the human enzyme is from erythrocytes. [b] Insoluble above stated concentration. [c] ND, not determined.

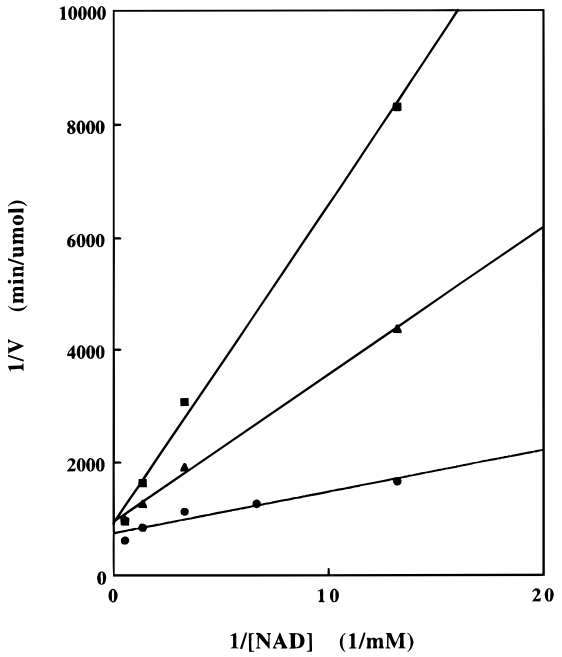

Figure 4. Competitive inhibition of *L. mexicana* GAPDH with 16 μM (triangles) and 32 μM (squares) **9a** versus the control (circles).

concentrations used to determine IC_{50} values. Statistical error limits on the IC_{50} values have been calculated and amount to 10%.

Molecular Modeling. Prior to synthesis, qualitative docking experiments were carried out with the program BIOGRAF[37] in conjunction with the Dreiding force field.[38] The adenosine moiety was fixed in the position observed in the crystal structure of *T. brucei*·NAD$^+$ [23] for the adenosyl portion of NAD$^+$. Substituents were then added to adenosine followed by conjugate gradient energy minimization (with the convergence criterion set to 0.1 kcal mol^{-1} Å^{-1}) in the presence of all enzyme residues within 12 Å of the modeled inhibitor. In all simulations the protein environment was kept rigid except where stated otherwise. Also, a water molecule hydrogen bonding to N^1 of adenosine, the main-chain N of Glu 90, and the ND2 of Asn 7 was included. The presence of this water molecule can be inferred by analogy with the crystal structure of *Bacillus stearothermophilus* GAPDH;[39] it is not visible in the *T. brucei* crystal structure due to the 3.2-Å resolution limit. Because energy calculations were performed in vacuo, the electrostatic potential energy function was turned off. The most important effect of electrostatics, namely, the formation of hydrogen bonds, was taken care of by explicit geometrical hydrogen bond potentials of the Lennard−Jones 12-10 type with angular dependence. This approach avoids the difficulties of calculating and calibrating charges for each new ligand and of treating dielectric effects in detail.[40]

For docking compounds **5b**−**f** the side-chain conformation of residue Met 38 was allowed to vary in order to alleviate short contacts between the CG atom and the aromatic ring of the 2′-ribosyl substituents. For docking compounds **9a**−**e** the side-chain conformations of residues Met 38, Leu 122, and Phe 113 were allowed to change to avoid short contacts. The latter two residues are the ones in contact with the N^6-purine substituents.

To check conformational preferences of several of our substituents, searches were carried out using the Cambridge Crystallographic Database,[41] followed by statistical analysis with the accompanying VISTA software.[42]

To examine the conformational energy difference between proximal and distal orientations of methyl with respect to the imidazole of N^6-methyladenine, their energies were calculated with the AM1 Hamiltoninan using the AMSOL 5.0 program.[43] Full geometry optimization was carried out.

Buried hydrophobic surface calculations were performed with the program NACCESS.[44]

Syntheses. 2′-Amino-2′-deoxy-3′,5′-*O*-(1,1,3,3-tetraisopropylsiloxane-1,3-diyl)adenosine (**3**) and N^6-(3-methyl-2-butenyl)-adenosine were synthesized as described.[30,45]

Protection of Hydroxy Acids. Hydroxybenzoic acids were protected via acetylation as described[27] in 80−95% yields, and the structures were verified by ^{1}H NMR.

2′-N-Acylation. Each of the acetoxybenzoic acids (150 mg) was suspended in 20 mL of dry CH_2Cl_2, and 100 mg of PCl_5 was added with stirring under Ar. The solution was stirred at room temperature for 5 h, then dried in vacuo overnight. To a solution of 30 mg of **3** in 10 mL of CH_2Cl_2/1 mL of pyridine, was added 3 equiv of acyl chloride, and the mixture was refluxed for 3 h under Ar. Reaction progress was monitored by TLC (10% MeOH/EtOAc: $R_f = 1$ for acyl chloride, 0.5 for product, and 0.05 for **3**). The solvent was evaporated; the solid was dried in vacuo and redissolved in EtOAc. The solution was extracted twice with saturated $NaHCO_3$, then dried, and chromatographed on silica. Nonpolar impurities were removed with EtOAc, and the product was eluted with 10% MeOH/AcOEt. R_f values for the derivatives are ∼0.4 using 100% EtOAc as solvent.

2′-Deoxy-2′-(3-methoxybenzamido)-3′,5′-*O*-(1,1,3,3-tetraisopropyldisiloxane-1,3-diyl)adenosine (4a). The described procedure with 10 mg (19.7 μmol) of **3** yielded 9.8 mg (77%) of the title compound: ^{1}H NMR δ 1−1.4 (m, 28, 4 *i*Pr), 3.85 (s, 3, OMe), 4.05−4.20 (m, 3, H4′,5′,5″), 4.95 (m, 1, H2′), 5.55 (m, 1, H3′), 6.16 (br s, 2, NH_2), 6.27 (d, 1, H1′), 7.08 (m, 1, H4), 7.26−7.40 (m, 3, H6″, 5″, 2″), 8.07 (s, 1, H2″), 8.26 (s, 1, H8); identical by NMR and TLC to the reported compound.[21]

2′-Deoxy-2′-(3-methoxy-4-acetoxybenzamido)-3′,5′-*O*-(1,1,3,3-tetraisopropyldisiloxane-1,3-diyl)adenosine (4b). The described procedure with 8 mg (15.7 μmol) of **3** yielded 11.4 mg (85%) of title compound: ^{1}H NMR δ 0.9−1.3 (m, 28, 4 *i*Pr), 2.33 (s, 3, acetate), 3.85 (s, 3, OMe), 4.05−4.15 (m, 3, H4′,5′,5″), 4.86 (m, 1, H2′), 5.57 (br s, 3, NH_2, H3′), 6.09 (d, 1, H1′), 7.11 (d, 1, H5″), 7.28 (dd, 1, H6″), 7.46 (d, 1, H2″), 8.01 (s, 1, H2), 8.26 (s, 1, H8).

2′-Deoxy-2′-(3-methoxy-2-acetoxybenzamido)-3′,5′-*O*-(1,1,3,3-tetraisopropyldisiloxane-1,3-diyl)adenosine (4c). The described procedure with 13.8 mg (27.2 μmol) of **3** yielded 6.6 mg (49%) product: ^{1}H NMR δ 0.9−1.4 (m, 28, 4 *i*Pr), 2.33 (s, 3, acetate), 3.82 (s, 3, OMe), 4.0−4.12 (m, 3, H4′,5′,5″), 4.86 (m, 1, H2′), 5.50 (m, 1, H3′), 6.00 (br s, 3, NH_2, H1′), 7.05−7.4 (m, 3, H4″, 5″, 6″), 7.96 (s, 1, H2), 8.2 (s, 1, H8).

2′-Deoxy-2′-(3-acetoxybenzamido)-3′,5′-*O*-(1,1,3,3-tetraisopropyldisiloxane-1,3-diyl)adenosine (4d). The described procedure with 10 mg (19.7 μmol) of **3** yielded 11 mg (85%) of title compound: ^{1}H NMR δ 0.85−1.3 (m, 28, 4 *i*Pr), 2.35 (s, 3, acetate), 4.04−4.15 (m, 3, H4′,5′,5″), 4.90 (m, 1, H2′),

5.55 (t, 1, H3′) 6.12 (d, 1, H1′), 6.40 (br s, 2, NH_2), 7.4−7.7 (m, 4, H2″, 4″, 5″, 6″), 8.05 (s, 1, H2), 8.27 (s, 1, H8).

2′-Deoxy-2′-(3,4,5-triacetoxybenzamido)-3′,5′-*O*-(1,1,3,3-tetraisopropyldisiloxane-1,3-diyl)adenosine (4e). The described procedure with 23 mg (45.3 μmol) of **3** yielded 15 mg (45%) of title compound: ^{1}H NMR δ 0.8−1.3 (m, 28, 4 *i*Pr), 2.25−2.31 (m, 9, acetates), 4.0−4.1 (m, 3, H4′,5′,5″), 4.84 (m, 1, H2′), 5.53 (t, 1, H3′), 5.59 (br s, 2, NH_2), 6.04 (d, 1, H1′), 7.52(s, 2, H2″, 6″), 7.96 (s, 1, H2), 8.24 (s, 1, H8).

2′-Deoxy-2′-(3,5-diacetoxybenzamido)-3′,5′-*O*-(1,1,3,3-tetraisopropyldisiloxane-1,3-diyl)adenosine (4f). The described procedure with 40 mg (78.7 μmol) of **3** yielded 33 mg (60%) of title compound: ^{1}H NMR δ 0.90−1.3 (m, 28, 4 *i*Pr), 2.28 (s, 6, acetates), 4.01−4.13 (m, 3, H4′,5′,5″), 4.85 (m, 1, H2′), 5.51 (t, 1, H3′) 6.05 (d, 1, H1′), 6.18 (br s, 2, NH_2), 7.09 (t, 1, H4″), 7.37 and 7.39 (s, 1 and 1, H2″, 6″), 7.99 (s, 1, H2), 8.21 (s, 1, H8).

2′-Deoxy-2′-(3-methoxy-4-hydroxybenzamido)adenosine (5b). Compound **4b** (8.8 mg, 13.4 μmol) was dissolved in 8 mL of 10% NH_3/MeOH and stirred for 15 min. The solution was dried and subjected to the NH_4F deprotection as described,[21] yielding 5.4 mg of **5b** (97%): ^{1}H NMR (DMSO-d_6) δ 3.58−3.72 (m, 2, H5′,5″), 3.76 (s, 3, OMe), 4.09 (m, 1, H4′), 4.29 (m, 1, H3′), 5.29 (m, 1, H2′), 5.61 (m, 1, 5′-OH), 5.76 (d, 1, 3′-OH), 6.17 (d, 1, H1′), 6.76 (d, 1, H5″), 7.28−7.35 (m, 2, H2″, 6″), 8.23 (br s, 2, NH_2), 8.09 (d, 1, NH), 8.11 (s, 1, H2), 8.23 (s, 1, H8).

2′-Deoxy-2′-(3-methoxy-2-hydroxybenzamido)adenosine (5c). The procedure for the synthesis of **5b** was followed for 8.8 mg of **4c** (13.4 μmol) and yielded 2.2 mg (40%) of **5c**: ^{1}H NMR (DMSO-d_6) δ 3.6−3.7 (m, 2, H5′,5″), 3.80 (s, 3, OMe), 4.10 (m, 1, H4′), 4.35 (m, 1, H3′), 5.32 (m, 1, H2′), 5.55−5.75 (m, 2, 3′,5′-OH), 6.12 (d, 1, H1′), 6.7−7.4 (3 m, 3, H4″, 5″, 6″), 7.30 (br s, 2, NH_2), 8.10 (s, 1, H2), 8.30 (s, 1, H8), 8.92 (d, 1, NH).

2′-Deoxy-2′-(3-hydroxybenzamido)adenosine (5d). The procedure for the synthesis of **5b** was followed for 11 mg of **4d** (16.8 μmol) and yielded 4.5 mg (70%) of **5d**: ^{1}H NMR (DMSO-d_6) δ 3.58−3.75 (m, 2, H5′,5″), 4.07 (br s, 1, H4′), 4.30 (t, 1, H3′), 5.25 (dd, 1, H2′), 5.63 (br s, 1, 5′-OH), 5.71 (d, 1, 3′-OH), 6.17 (d, 1, H1′), 6.87 (m, 1, H4″), 7.15−7.22 (m, 3, H2″, 5″, 6″), 7.35 (br s, 2, NH_2), 8.10 (s, 1, H2), 8.16 (d, 1, NH), 8.23 (s, 1, H8).

2′-Deoxy-2′-(3,4,5-trihydroxybenzamido)adenosine (5e). The procedure for the synthesis of **5b** was followed for 6 mg of **4e** (9.5 μmol) and yielded 3.8 mg (96%) of **5e**: ^{1}H NMR (MeOH-d_4) δ 3.75−3.92 (m, 2, H5′, 5″), 4.23 (br s, 1, H4′), 4.47 (m, 1, H3′), 5.80 (dd, 1, H2′), 6.11 (d, 1, H1′), 6.70 (s, 2, H2″, 6″), 8.17 (s, 1, H2), 8.27 (s, 1, H8).

2′-Deoxy-2′-(3,5-dihydroxybenzamido)adenosine (5f). The procedure for the synthesis of **5b** was followed for 5 mg of **4f** (7.2 μmol) and yielded 2.5 mg (86%) of **5f**: ^{1}H NMR (DMSO-d_6) δ 3.60−3.75 (m, 2, H5′,5″), 4.08 (br s, 1, H4′), 4.30 (t, 1, H3′), 5.21 (dd, 1, H2′), 5.63 (br s, 1, 5′-OH), 5.69 (d, 1, 3′-OH), 6.16 (d, 1, H1′), 6.32 (br s, 1, H4″), 6.61 (br s, 2, H2″, 6″), 7.33 (br s, 2, NH_2), 8.00 (d, 1, NH), 8.13 (s, 1, H2), 8.23 (s, 1, H8).

N^6-Acylation. *N*^{6}-Isobutyryl-2′-deoxy-2′-(3-methoxybenzamido)adenosine (6a). Compound **4a** (9 mg, 14 μmol) was dissolved in 10 mL of 50% CH_2Cl_2/50% pyridine, and 30 μL (0.29 mmol) of isobutyryl chloride was added. The mixture was kept at room temperature for 14 h, and solvent was removed in vacuo. The resulting oil was pure by TLC (R_f 0.5 in EtOAc) and was subjected to NH_4F deprotection procedure in MeOH at 45 °C overnight. The product was chromatographed on silica (10−15% MeOH/EtOAc): yield 4.5 mg (45%); ^{1}H NMR (MeOH-d_4) δ 1.1−1.2 (d, 6, 2 Me), 2.9 (m, 1, CH), 3.80 (s, 3, OMe), 4.8−4.95 (m, 2, H5′,5″), 4.27 (m, 1, H4′), 4.51 (dd, 1, H3′), 5.35 (dd, 1, H2′), 6.30 (d, 1, H1′), 7.0−7.5 (m, 4, aromatic protons), 8.56−8.62 (s, 1, H8 and s, 1, H2).

N^6-Coupling. All *N*^{6}-alkyladenosines were synthesized from 6-chloropurine riboside and the corresponding amines under the conditions described by Fleysher in 90−100% yield.[28,29]

***N*^{6}-Isopropyladenosine (7a):** ^{1}H NMR (MeOH-d_4) δ 1.27−1.32 (d of d, 6, 2 CH_3), 3.40 (m, 1, CH), 3.68−3.90 (m, 2, H5′, 5″), 4.18 (m, 1, H4′), 4.30 (dd, 1, H3′), 4.71 (dd, 1, H2′), 5.91 (d, 1, H1′), 8.18−8.24 (2 s, 2, H8, 2); ESI-MS (methanol) 310.2 $(M + H)^+$.

***N*^{6}-*tert*-Butyladenosine (7b):** ^{1}H NMR (MeOH-d_4) δ 1.38 (s, 6, 2 CH_3), 1.62 (s, 3, CH_3), 3.70−3.95 (m, 2, H5′,5″), 4.20 (m, 1, H4′), 4.32 (m, 1, H3′), 4.77 (dd, 1, H2′), 5.94 (d, 1, H1′), 8.20−8.24 (s, 2, H8, 2); ESI-MS (methanol) 324.2 $(M + H)^+$.

***N*^{6}-Amyladenosine (7c):** ^{1}H NMR (MeOH-d_4) δ 0.9 (m, 3, CH_3), 1.3 (m, 4, γ,δ CH_2), 1.65 (m, 2, β-CH_2), 3.57 (m, 2, α-CH_2), 3.65−3.9 (m, 2, H5′, 5″), 4.15 (m, 1, H4′), 4.28 (dd, 1, H3′), 4.75 (dd, 1, H2′), 5.90 (d, 1, H1′), 8.1−8.2 (2 s, 2, H8, 2); ESI-MS (methanol) 338.2 $(M + H)^+$.

***N*^{6}-(2-Amyl)adenosine (7d):** ^{1}H NMR (MeOH-d_4) δ 0.97 (dd, 3, CH_3), 1.27 (dd, 3, CH_3), 1.43 (m, 2, CH_2), 1.59 (m, 2, CH_2), 3.29 (m, 1, CH), 3.70−3.94 (m, 2, H5′, 5″), 4.18 (dd, 1, H4′), 4.32 (dd, 1, H3′), 4.76 (dd, 1, H2′), 5.95 (d, 1, H1′), 8.18−8.23 (2 s, 2, H8, 2); ESI-MS (methanol) 338.2 $(M + H)^+$.

***N*^{6}-(2-Methylbutyl)adenosine (7e):** ^{1}H NMR (MeOH-d_4) δ 0.92−1.07 (m, 6, 2 CH_3), 1.28 (m, 1, γ-CH_2), 1.51 (m, 1, γ-CH_2), 1.78 (m, 1, CH), 2.72 (dd, 1, α-CH_2), 2.90 (dd, 1, α-CH_2), 3.70−3.93 (m, 2, H5′, 5″), 4.20 (dd, 1, H4′), 4.34 (dd, 1, H3′), 4.76 (dd, 1, H2′), 5.97 (d, 1, H1′), 8.20−8.26 (2 s, 2, H8, 2); ESI-MS (methanol) 338.2 $(M + H)^+$.

***N*^{6}-Isoamyladenosine (7f):** ^{1}H NMR (MeOH-d_4) δ 1.0 (d, 6, 2 CH_3), 1.62 (m, 2, β-CH_2), 1.72 (m, 1, CH), 2.88 (m, 2, α-CH_2), 3.7−3.95 (m, 2, H5′, 5″), 4.20 (m, 1, H4′), 4.32 (dd, 1, H3′), 4.74 (dd, 1, H2′), 5.94 (d, 1, H1′), 8.20−8.25 (2 s, 2, H8, 2); ESI-MS (methanol) 338.3 $(M + H)^+$.

***N*^{6}-Cyclopentyladenosine (7h):** ^{1}H NMR (MeOH-d_4) δ 1.70 (m, 4, 2 β-CH_2), 2.10 (m, 4, 2 α-CH_2), 3.58 (m, 1, CH), 3.70−3.93 (m, 2, H5′, 5″), 4.19 (dd, 1, H4′), 4.33 (dd, 1, H3′), 4.75 (dd, 1, H2′), 5.94 (d, 1, H1′), 8.20−8.25 (2 s, 2, H8, 2); ESI-MS (methanol) 336.2 $(M + H)^+$.

***N*^{6}-Cycloheptyladenosine (7i):** ^{1}H NMR δ 1.3−2.0 (m, 12, aliphatic protons), 3.0 (m, 1, α-CH), 3.7−3.9 (m, 2, H5′, 5″), 4.25 (m, 1, H4′), 4.35 (dd, 1, H3′), 4.90 (dd, 1, H2′), 5.77 (d, 1, H1′), 5.94 (br s, 1, NH), 7.80 (s, 1, H2), 8.20 (s, 1, H8); ESI-MS (methanol) 364.3 $(M + H)^+$.

***N*^{6}-(2-Methylbenzyl)adenosine (7j):** ^{1}H NMR (MeOH-d_4) δ 2.4 (s, 3, CH_3), 3.7−3.9 (m, 2, H5′, 5″), 4.15 (m, 1, H4′), 4.31 (dd, 1, H3′), 4.77 (dd, 1, H2′), 5.94 (d, 1, H1′), 7.1−7.4 (m, 4, aromatic protons), 8.22 (2 s, 2, H8, 2); ESI-MS (methanol) 372.3 $(M + H)^+$.

***N*^{6}-(3-Methylbenzyl)adenosine (7k):** ^{1}H NMR (MeOH-d_4) δ 2.32 (s, 3, CH_3), 3.7−3.9 (m, 2, H5′, 5″), 3.87 (s, 2, CH_2), 4.18 (m, 1, H4′), 4.31 (dd, 1, H3′), 4.75 (dd, 1, H2′), 5.93 (d, 1, H1′), 6.95−7.2 (m, 4, aromatic protons), 8.2 (2 s, 2, H8, 2); ESI-MS (methanol) 372.3 $(M + H)^+$.

***N*^{6}-(1,2,3,4-Tetrahydro-1-naphthyl)adenosine (7l):** ^{1}H NMR δ 1.8−2.4 (m, 6, H2″, H3″, H4″), 3.65−3.95 (m, 2, H5′, 5″), 4.14 (m, 1, H4′), 4.29 (m, 1, H3′), 4.4 (m, 1, H1″), 4.98 (m, 1, H2′), 5.75 (d, 1, H1′), 6.20 (br s, 1, NH), 7.0−7.2 (m, 4, H5″, 6″, 7″, 8″), 7.70 (s, 1, H2), 8.28 (s, 1, H8); ESI-MS (methanol) 398.2 $(M + H)^+$.

***N*^{6}-(1-Naphthalenemethyl)adenosine (7m):** ^{1}H NMR δ 3.7−3.95 (m, 2, H5′, 5″), 4.20 (m, 1, H4′), 4.33 (m, 1, H3′), 4.40 (s, 2, CH_2), 4.78 (m, 1, H2′), 5.93 (d, 1, H1′), 7.4−8.1 (m, 7, aromatic protons), 8.19−8.23 (2 s, 2, H8, 2); ESI-MS (methanol) 408.1 $(M + H)^+$.

***N*^{6}-[2-(2-(Hydroxymethyl)phenylthio)benzyl]adenosine (7n):** ^{1}H NMR δ 3.71−3.91 (m, 2, H5′, H5″), 4.18 (m, 1, H4′), 4.31 (dd, 1, H3′), 4.70 (s, 2, CH_2O), 4.73 (dd, 1, H2′), 4.90 (br s, 2, CH_2N), 5.91 (d, 1, H1′), 7.05−7.50 (m, 8, aromatic protons), 8.15−8.25 (2 s, 2, H8, 2); ESI-MS (methanol) 496.2 $(M + H)^+$.

***N*^{6}-(Diphenylmethyl)adenosine (7o):** ^{1}H NMR (MeOH-d_4) δ 3.7−3.9 (m, 2, H5′, 5″), 4.17 (m, 1, H4′), 4.29 (dd, 1, H3′), 4.72 (dd, 1, H2′), 5.34 (s, 1, CH), 5.92 (d, 1, H1′), 7.2−7.35 (m,

10, aromatic protons), 8.17 (s, 1, H2), 8.26 (s, 1, H8); ESI-MS 434.0 $(M + H)^+$.

N^6-Alkylation. N^6-Benzyl-2′-deoxy-2′-(3-methoxybenzamido)-3′,5′-*O*-(1,1,3,3-tetraisopropyldisiloxane-1,3-diyl)adenosine (8a). Benzyl bromide (0.12 mL, 1 mmol) was added to a solution of 24 mg (37.4 μmol) of **4a** in 5 mL of DMF, and the mixture was kept at 45 °C for 14 h until no starting material could be detected by TLC (EtOAc). DMF was evaporated in vacuo, and the remaining oil was dried by coevaporation with MeOH. It was then dissolved in 25% ^{i}PrNH$_2$/75% MeOH and slowly refluxed for 24 h. The solid was dried and chromatographed on silica with 1:1 hexane/EtOAc (R_f 0.7 in EtOAc): yield 14.3 mg (52%); ^{1}H NMR δ 0.85−1.2 (m, 28, 4 *i*Pr), 3.81 (s, 3, OMe), 3.89−4.15 (m, 2, H5′, 5″), 4.25 (d, 1, H4′), 4.80 (m, 3, H2′, CH$_2$), 5.26 (t, 1, H3′), 6.12 (d, 1, H1′), 6.43 (br s, 1, NH amine), 7.2−7.4 (m, 9, aromatic protons), 8.02 (s, 1, H2), 8.34 (s, 1, H8).

N^6-(3-Methyl-2-butenyl)adenosine (7g). 4-Bromo-2-methyl-2-butene (0.05 mL, 0.43 mmol) was added to a solution of 30 mg (112 μmol) of adenosine and 35 mg of $BaCO_3$ in 5 mL of DMF, and the mixture stirred at room temperature in the dark for 48 h. DMF was evaporated in vacuo, and the rearrangement was performed in a similar manner as for **10a** yielding 11.8 mg (31%) of title compound: ^{1}H NMR δ 1.7 (br s, 6, 2 δ-CH$_3$), 3.65−3.95 (m, 2, H5′, 5″), 4.15 (m, 1, H4′), 4.30 (m, 1, H3′), 4.15 and 4.40 (m, 2, α-CH$_2$), 5.0 (m, 1, H2′), 5.30 (t, 1, β-CH) 5.78 (d, 1, H1′), 6.0 (br s, 1, NH), 7.75 (s, 1, H2), 8.05 (s, 1, H8); ESI-MS (methanol) 336.3 $(M + H)^+$.

N^6-Benzyl-2′-deoxy-2′-(3-methoxybenzamido)adenosine (9a). Deprotection procedure described for **1**[21] starting with 2.1 mg (4.3 μmol) of **8a** gave quantitative yield of product, which was purified on silica (R_f 0.25 in EtOAc) and on a C$_{18}$ Sep-Pak cartridge (loaded in MeOH/H$_2$O and eluted with MeOH): ^{1}H NMR (DMSO-d_6) δ 3.58−3.72 (m, 2, H5′, 5″), 3.76 (s, 3, OMe), 4.08 (m, 1, H4′), 4.32 (m, 1, H3′), 4.68 (br s, 2, CH$_2$), 5.30 (m, 1, H2′), 5.57 (dd, 1, 5′-OH), 5.72 (d, 1, 3′-OH), 6.21 (d, 1, H1′), 7.1−7.4 (m, 9, aromatic protons), 8.17 (s, 1, H2), 8.27 (s, 1, H8), 8.33 (d, 1, NH amide); ESI-MS (methanol) 491.2 $(M + H)^+$.

N^6-(2-Methylbenzyl)-2′-deoxy-2′-(3-methoxybenzamido)-adenosine (9b). The procedures for **8a** and **9a** were applied in sequence using 15.6 mg (24.3 μmol) of **4a** and 0.12 mL (166 mg, 0.9 mmol) of 2-methylbenzyl bromide. The overall yield for the two steps was 0.7 mg (6%): ^{1}H NMR (DMSO-d_6) δ 2.32 (s, 3, CH$_3$), 3.6−3.75 (m, 2, H5′, 5″), 3.79 (s, 3, OMe), 4.10 (m, 1, H4′), 4.32 (m, 1, H3′), 4.65 (br s, 2, CH$_2$), 5.30 (m, 1, H2′), 5.59 (dd, 1, 5′-OH), 5.72 (d, 1, 3′-OH), 6.21 (d, 1, H1′), 7.05−7.45 (m, 8, aromatic protons), 8.18 (s, 1, H2), 8.29 (s, 1, H8), 8.34 (d, 1, NH amide); ESI-MS (methanol) 505.3 $(M + H)^+$.

N^6-(2-Methoxybenzyl)-2′-deoxy-2′-(3-methoxybenzamido)adenosine (9c). The overall yield for the two steps was 38%: ^{1}H NMR (MeOH-d_4) δ 3.81 (m, 1, H5′), 3.92 (m, 1, H5″), 3.79, 3.86 (2 s, 6, 2 OMe), 4.28 (m, 1, H4′), 4.50 (m, 1, H3′), 4.77 (br s, 2, CH$_2$), 5.38 (m, 1, H2′), 6.19 (d, 1, H1′), 6.85−7.30 (m, 8, aromatic protons), 8.22 (2 s, 2, H8, 2); ESI-MS (methanol) 521.4 $(M + H)^+$.

N^6-(2,5-Dimethylbenzyl)-2′-deoxy-2′-(3-methoxybenzamido)adenosine (9d). The overall yield for the two steps was 25%: ^{1}H NMR (DMSO-d_6) δ 2.13, 2.27 (2 s, 6, 2 CH$_3$), 3.58−3.75 (m, 2, H5′, 5″), 3.76 (s, 3, OMe), 4.09 (m, 1, H4′), 4.32 (m, 1, H3′), 4.61 (br s, 2, CH$_2$), 5.30 (m, 1, H2′), 5.59 (dd, 1, 5′-OH), 5.73 (d, 1, 3′-OH), 6.21 (d, 1, H1′), 6.9−7.45 (m, 7, aromatic protons), 8.19 (s, 1, H2), 8.29 (s, 1, H8), 8.36 (d, 1, NH amide); ESI-MS (methanol) 519.3 $(M + H)^+$.

N^6-(2,3-Dimethylbenzyl)-2′-deoxy-2′-(3-methoxybenzamido)adenosine (9e). The overall yield for the two steps was 11%: ^{1}H NMR (MeOH-d_4) δ 2.26, 2.29 (2 s, 6, 2 CH$_3$), 3.79 (s, 3, OMe), 3.8−3.93 (m, 2, H5′, 5″), 4.27 (m, 1, H4′), 4.5 (m, 1, H3′), 4.75 (br s, 2, CH$_2$), 5.38 (m, 1, H2′), 6.2 (d, 1, H1′), 7.0−7.35 (m, 7, aromatic protons), 8.22−8.27 (2 s, 2, H8,2); ESI-MS (methanol) 519.3 $(M + H)^+$.

Acknowledgment. This work was supported by Grant HL36235 from the National Institutes of Health to M.H.G. A.M.A. is the recipient of a Dow Chemical Fellowship Award. We wish to thank Drs. Paul A. Michels and Hidong Kim for providing a source of enzyme and Murdock Charitable Trust for a major equipment grant to the University of Washington Biomolecular Structure Center.

References

(1) WHO Consultation Program. *Bull. W. H. O.* **1982**, *60*, 821−825.
(2) Clayton, C.; Haeusler, T.; Blattner, J. Protein Trafficking in Kinetoplastid Protozoa. *Microbiol. Rev.* **1995**, *59*, 325−344.
(3) Despommier, D. D.; Gwadz, R. W.; Hotez, P. J. *Parasitic Diseases*; Springer-Verlag: New York, 1995; pp 196−203.
(4) Meshnick, S. R. In *Parasitic Diseases*; Mansfield, J. M., Ed.; Marcel Dekker: New York, 1984; Vol. 2, pp 165−199.
(5) Rew, R. S. Protozoan Infections of Man: African Trypanosomiasis. In *Chemotherapy of Parasitic Diseases*; Campbell, W. C., Rew, R. S., Eds.; Plenum: New York, 1986; pp 129−138.
(6) Bitonti, A. J.; Byers, T. L.; Bush, T. L.; Casara, P. J.; Bacchi, C. J.; Clarkson, J.; McCann, P. P.; Sjoerdsma, A. Cure of *Trypanosoma brucei* brucei and *Trypanosoma brucei rhodesiense* Infections in Mice with an Irreversible Inhibitor of S-Adenosylmethionine Decarboxylase. *Antimicrob. Agents Chemother.* **1990**, *34*, 1485−1490.
(7) Bacchi, C. J.; Nathan, H. C.; Yarlett, N.; Goldberg, B.; McCann, P. P.; Sjoerdsma, A.; Saric, M.; Clarkson, A. B., Jr. Combination Chemotherapy of Drug-Resistant *Trypanosoma brucei rhodesiense* Infections in Mice Using DL-α-Difluoromethylornithine and Standard Trypanocides. *Antimicrob. Agents Chemother.* **1994**, *34*, 563−569.
(8) Gutteridge, W. E. Existing Chemotherapy and its Limitations. *Br. Med. Bull.* **1985**, *41*, 162−168.
(9) Metcalf, B. W.; Bey, P.; Danzin, C.; Jung, M. J.; Casara, P.; Vevert, J. P. Catalytic Irreversible Inhibition of Mammalian Ornithine Decarboxylase (4.1.1.17) by Substrate and Product Analogues. *J. Am. Chem. Soc.* **1978**, *100*, 2551−2553.
(10) Schechter, P. J.; Barlow, J. R. L.; Sjoerdsma, A. Clinical Aspects of Inhibition of Ornithine Decarboxylase with Emphasis on Therapeutic Trials of Eflornithine (DFMO) in Cancer and Protozoan Disease. In *Inhibition of Polyamine Metabolism*; McCann, P. P., Pegg, A. E., Sjoerdsma, A., Eds.; Academic: New York, 1987; pp 345−364.
(11) *Trop. Drug Res. News* **1990**, *34*, 1.
(12) Bellofatto, V.; Fairlamb, A.; Henderson, G. B.; Cross, G. A. M. Biochemical changes associated with α-difluoromethylornithine uptake and resistance in *Trypanosoma brucei*. *Mol. Biochem. Parasitol.* **1987**, *25*, 227−238.
(13) Opperdoes, F. R. Biochemical Peculiarities of Trypanosomes, African and South American. *Br. Med. Bull.* **1985**, *41*, 130−136.
(14) Opperdoes, F. R. Compartmentation of Carbohydrate Metabolism in Trypanosomes. *Annu. Rev. Microbiol.* **1987**, *41*, 127−151.
(15) Clarkson, A. B., Jr.; Brohn, F. H. Trypanosomiasis: An Approach to Chemotherapy by the Inhibition of Carbohydrate Catabolism. *Science* **1976**, *194*, 204−206.
(16) Lambeir, A.-M.; Loiseau, A. M.; Kuntz, D. A.; Vellieux, F. M.; Michels, P. A. M.; Opperdoes, F. R. The cytosolic and glycosomal glyceraldehyde-3-phosphate dehydrogenase from *Trypanosoma brucei*. Kinetic properties and comparison with homologous enzymes. *Eur. J. Biochem.* **1991**, *198*, 429−435.
(17) Bakker, B. M.; Michels, P. A. M.; Opperdoes, F. R.; Westerhoff, H. V. Glycolysis in Bloodstream Form *Trypanosoma brucei* Can Be Understood in Terms of the Kinetics of the Glycolytic Enzymes. *J. Biol. Chem.* **1997**, *272*, 3207−3215.
(18) Eisenthal, R.; Cornish-Bowden, A. Prospects for Antiparasitic Drugs. *J. Biol. Chem.* **1998**, *273*, 5500−5505.
(19) Bakker, B. M. Control and Regulation of Glycolysis in *Trypanosoma brucei*. Ph.D. Thesis, Free University of Amsterdam, 1998.
(20) Verlinde, C. L. M. J.; Callens, M.; Van Calenbergh, S.; Van Aerschot, A.; Herdewijn, P.; Hannaert, V.; Michels, P. A. M.; Opperdoes, F. R.; Hol, W. G. J. Selective Inhibition of Trypanosomal Glyceraldehyde-3-Phosphate Dehydrogenase by Protein Structure-Based Design: Toward New Drugs for the Treatment of Sleeping Sickness. *J. Med. Chem.* **1994**, *37*, 3605−3613.
(21) Van Calenbergh, S.; Van Den Eeckhout, E.; Herdewijn, P.; De Bruyn, A.; Verlinde, C.; Hol, W.; Callens, M.; Van Aerschot, A.; Rozenski, J. Synthesis and Conformational Analysis of 2′-Deoxy-2′-(3-methoxybenzamido)adenosine, a Rational-Designed Inhibitor of Trypanosomal Glyceraldehyde Phosphate Dehydrogenase (GAPDH). *Helv. Chim. Acta* **1994**, *77*, 631−644.
(22) Van Calenbergh, S.; Verlinde, C. L. M. J.; Soenens, J.; De Bruyn, A.; Callens, M.; Blaton, N. M.; Peeters, O. M.; Rozenski, J.; Hol, W. G. J.; Herdewijn, P. Synthesis and Structure−Activity

Relationships of Analogues of 2′-Deoxy-2′-(3-methoxybenzamido)adenosine, a Selective Inhibitor of Trypanosomal Glycosomal Glyceraldehyde-3-phosphate Dehydrogenase. *J. Med. Chem.* **1995**, *38*, 3838−3849.

(23) Vellieux, F. M. D.; Hajdu, J.; Verlinde, C. L. M. J.; Groendijk, H.; Read, R. J.; Greenhough, T. J.; Campbell, J. W.; Kalk, K. H.; Littlechild, J. A.; Watson, H. C.; Hol, W. G. J. Structure of glycosomal glyceraldehyde-3-phosphate dehydrogenase from *Trypanosoma brucei* determined from Laue data. *Proc. Natl. Acad. Sci. U.S.A.* **1993**, *90*, 2355−2359.

(24) Willson, M.; Lauth, N.; Perie, J.; Callens, M.; Opperdoes, F. R. Inhibition of Glyceraldehyde-3-Phosphate Dehydrogenase by Phosphorylated Epoxides and α-Enones. *Biochemistry* **1994**, *33*, 214−220.

(25) Saenger, W. *Principles of Nucleic Acid Structure*; Springer-Verlag: New York, 1984.

(26) Robins, M. J.; Wilson, J. S.; Hansske, F. Nucleic Acid Related Compounds. 42. A General Procedure for the Efficient Deoxygenation of Secondary Alcohols. Regiospecific and Stereoselective Conversion of Ribonucleosides to 2′-Deoxynucleosides. *J. Am. Chem. Soc.* **1983**, *105*, 4059−4065.

(27) White, B. B.; Barabash, E. U.S. Patent 2 581 565, 1952; *Chem. Abstr.* **1952**, *46*, 5842.

(28) Fleysher, M. H.; Hakala, M. T.; Bloch, A.; Hall, R. H. Synthesis and Biological Activity of Some N6−Alkyladenosines. *J. Med. Chem.* **1968**, *11*, 717−720.

(29) Fleysher, M. H. N6-Substituted Adenosines: Synthesis, Biological Activity, and Some Structure−Activity Relationships. *J. Med. Chem.* **1972**, *15*, 187−191.

(30) Robins, M. J.; Trip, E. M. Sugar-Modified N6-(3-Methyl-2-butenyl)adenosine Derivatives, N6-Benzyl analogues, and Cytokinin-Related Nucleosides Containing Sulfur or Formycin. *Biochemistry* **1973**, *12*, 2179−2187.

(31) Drew, J.; Letellier, M.; Morand, P.; Szabo, A. G. Synthesis from Pregnenolone of Fluorescent Cholesterol Analogue Probes with Conjugated Unsaturation in the Side Chain. *J. Org. Chem.* **1987**, *52*, 4047−4052.

(32) Raederstorff, D.; Shu, A. Y. L.; Thompson, J. E.; Djerassi, C. Biosynthetic Studies of Marine Lipids. 11. Synthesis, Biosynthesis, and Absolute Configuration of the Internally Branched Demospongic Acid, 22-Methyl-5,9-Octacosadienoic acid. *J. Org. Chem.* **1987**, *52*, 2337−2346.

(33) Kim, H.; Feil, I.; Verlinde, C. L. M. J.; Petra, P. H.; Hol, W. G. J. Crystal Structure of Glycosomal Glyceraldehyde-3-Phosphate Dehydrogenase from *Leishmania Mexicana*: Implications for Structure-Based Drug Design and a New Position for the Inorganic Phosphate Binding Site. *Biochemistry* **1995**, *34*, 14975−14986.

(34) Quideau, S.; Feldman, K. S.; Appel, H. M. Chemistry of Galloyl-Derived o-Quinones: Reactivity Toward Nucleophiles. *J. Org. Chem.* **1995**, *60*, 4982−4983.

(35) Harvey, R. G. Polycyclic Hydrocarbons and Carcinogenesis. *ACS Monograph No. 283*; American Chemical Society: Washington, DC, 1985.

(36) Hannaert, V.; Opperdoes, F. R.; Michels, P. A. M. Glycosomal Glyceraldehyde-3-Phosphate Dehydrogenase of *Trypanosoma brucei* and *Trypanosoma cruzi*: Expression in *Escherichia coli*, Purification and Characterization of the Enzymes. *Protein Expr. Purif.* **1995**, *6*, 244−250.

(37) Molecular Simulations Inc., Biograf 3.10; San Diego, CA.

(38) Mayo, S. L.; Olafson, B. D.; Goddard, W. A., III. DREIDING: A Generic Force Field for Molecular Simulations. *J. Phys. Chem.* **1990**, *94*, 8897−8909.

(39) Skarzynski, T.; Moody, P. C. E.; Wonacott, A. J. Structure of the holo-glyceraldehyde-3-phosphate dehydrogenase from *Bacillus stearothermophilus* at 1.8 A resolution. *J. Mol. Biol.* **1987**, *193*, 171−187.

(40) Mueller, K.; Amman, H.-J.; Doran, D.; Gerber, P. R.; Gubernator, K.; Schrepfer, G. The Use of Computer Modeling and Structural Databases in Pharmaceutical Research. In *Trends in Medicinal Chemistry '88*; van der Goot, H., Domany, G., Pallos, L., Timmerman, H., Eds.; Elsevier Science Publishers: Amsterdam, 1989; pp 1−12.

(41) Allen, F. H.; Davies, J. E.; Galloy, J. J.; Johnson, O.; Kennard, O.; Macrea, C. F.; Mitchell, E. M.; Mitchell, G. F.; Smith, M. J.; Watson, D. G. The Development of Versions 3 and 4 of the Cambridge Crystallographic Database System. *J. Chem. Inf. Comput. Sci.* **1993**, *31*, 187−204.

(42) Watson, D. G. The Cambridge Structural Database (CSD): Current Activities and Future Plans. *J. Res. Natl. Inst. Stand. Technol.* **1996**, *101*, 227−229.

(43) Liotard, D. A.; Hawkins, G. D.; Lynch, G. C.; Cramer, C. J.; Truhlar, D. G. Improved Methods for Semiempirical Solvation Models. *J. Comput. Chem.* **1995**, *16*, 422−440.

(44) Hubbard, S. J.; Thornton, J. M. NACCESS, London.

(45) Robins, M. J.; Hawrelak, S. D.; Hernandez, A. E.; Wnuk, S. F. Nucleic Acid Related Compounds. 71. Efficient General Synthesis of Purine (Amino, Azido, and Triflate)-Sugar Nucleosides. *Nucleosides Nucleotides* **1992**, *11*, 821−834.

JM9802620